3 FRACTURE MECHANICS

3.1 INTRODUCTION

The fatigue life of a component is made up of initiation and propagation stages. This is illustrated schematically in Fig. 3.1. The size of the crack at the transition from initiation to propagation is usually unknown and often depends on the point of view of the analyst and the size of the component being analyzed. For example, for a researcher equipped with microscopic equipment it may be on the order of a crystal imperfection, dislocation, or a 0.1 mm-crack, while to the inspector in the field it may be the smallest crack that is readily detectable with nondestructive inspection equipment. Nevertheless, the distinction between the initiation life and propagation life is important. At low strain amplitudes up to 90% of the life may be taken up with initiation, while at high amplitudes the majority of the fatigue life may be spent propagating a crack. Fracture mechanics approaches are used to estimate the propagation life.

Fracture mechanics approaches require that an initial crack size be known or assumed. For components with imperfections or defects (such as welding porosities, inclusions and casting defects, etc.) an initial crack size may be known. Alternatively, for an estimate of the total fatigue life of a defect-free material, fracture mechanics approaches can be used to determine propagation. Strain–life approaches may then be used to determine initiation life, with the total life being the sum of these two estimates.

In this chapter we briefly review the fundamentals of fracture mechanics and discuss the use of these concepts in applications to constant amplitude fatigue crack propagation analyses. In Chapter 4 we review fracture mechanics ap-

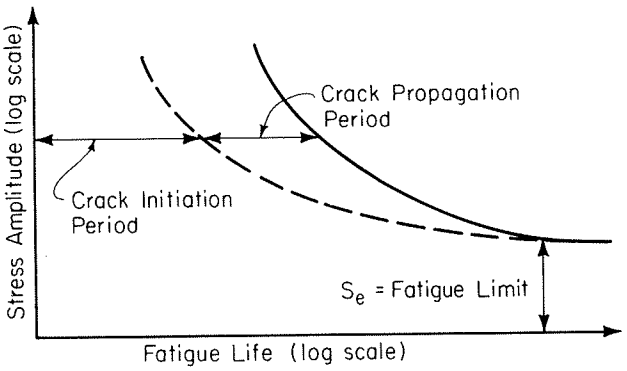

Figure 3.1 Initiation and propagation portions of fatigue life.

proaches for the analysis of notched components and in Chapter 5 discuss fracture mechanics approaches used to predict fatigue crack growth under variable amplitude loading.

3.2 LINEAR ELASTIC FRACTURE MECHANICS BACKGROUND

Linear elastic fracture mechanics (LEFM) principles are used to relate the stress magnitude and distribution near the crack tip to:

- Remote stresses applied to the cracked component
- The crack size and shape
- The material properties of the cracked component

3.2.1 Historical Overview

In the 1920s, Griffith [1] formulated the concept that a crack in a component will propagate if the total energy of the system is lowered with crack propagation. That is, if the change in elastic strain energy due to crack extension is larger than the energy required to create new crack surfaces, crack propagation will occur.

Griffith's theory was developed for brittle materials. In the 1940s, Irwin [2] extended the theory for ductile materials. He postulated that the energy due to plastic deformation must be added to the surface energy associated with the creation of new crack surfaces. He recognized that for ductile materials, the surface energy term is often negligible compared to the energy associated with plastic deformation. Further, he defined a quantity, G, the strain energy release rate or "crack driving force," which is the total energy absorbed during cracking per unit increase in crack length and per unit thickness.

In the mid-1950s, Irwin [3] made another significant contribution. He

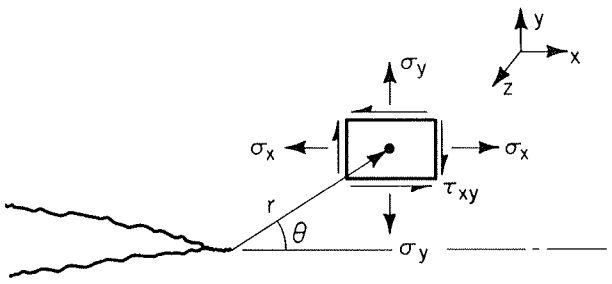

Figure 3.2 Location of local stresses near a crack tip in cylindrical coordinates.

showed that the local stresses near the crack tip are of the general form

$$\sigma_{ij} = \frac{K}{\sqrt{2\pi r}} f_{ij}(\theta) + \cdots \tag{3.1}$$

where r and θ are cylindrical coordinates of a point with respect to the crack tip (see Fig. 3.2) and K is the stress intensity factor. He further showed that the energy approach (the "G" approach above) is equivalent to the stress intensity approach (described in Section 3.2.4) and that crack propagation occurs when a critical strain energy release rate, G_c (or in terms of a critical stress intensity, K_c) is achieved.

3.2.2 LEFM Assumptions

Linear elastic fracture mechanics (LEFM) is based on the application of the theory of elasticity to bodies containing cracks or defects. The assumptions used in elasticity are also inherent in the theory of LEFM: namely, small displacements and general linearity between stresses and strains.

The general form of the LEFM equations is given in Eq. (3.1). As seen, a singularity exists such that as r, the distance from the crack tip, tends toward zero, the stresses go to infinity. Since materials plastically deform as the yield stress is exceeded, a plastic zone will form near the crack tip. The basis of LEFM remains valid, though, if this region of plasticity remains small in relation to the overall dimensions of the crack and cracked body.

3.2.3 Loading Modes

There are generally three modes of loading, which involve different crack surface displacements (see Fig. 3.3). The three modes are:

Mode I: opening or tensile mode (the crack faces are pulled apart)

Mode II: sliding or in-plane shear (the crack surfaces slide over each other)

Mode III: tearing or anti-plane shear (the crack surfaces move parallel to the leading edge of the crack and relative to each other)

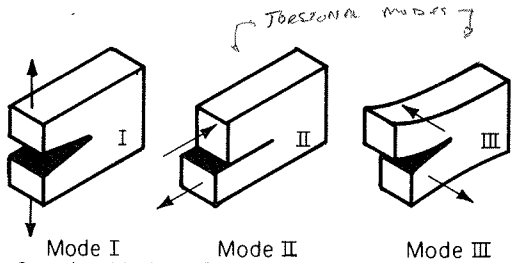

Figure 3.3 Three loading modes.

The following discussion deals with Mode I since this is the predominant loading mode in most engineering applications. Similar treatments can readily be extended to Modes II and III. Equations and additional details are found in Refs. 4 to 6.

3.2.4 Stress Intensity Factor

The stress intensity factor, K, which was introduced in Eq. (3.1), defines the magnitude of the local stresses around the crack tip. This factor depends on loading, crack size, crack shape, and geometric boundaries, with the general form given by

$$K = f(g)\sigma\sqrt{\pi a} \tag{3.2}$$

where σ = remote stress applied to component [not to be confused with the local stresses, σ_{ij}, in Eq. (3.1)]
a = crack length
$f(g)$ = correction factor that depends on specimen and crack geometry

Stress intensity factor solutions have been obtained for a wide variety of problems and published in handbook form [7–9]. Figure 3.4 gives the stress intensity relationships for a few of the more common loading conditions.

Stress intensity factors for a single loading mode can be added algebraically. Consequently, stress intensity factors for complex loading conditions of the same mode can be determined from the superposition of simpler results, such as those readily obtainable from handbooks.

One superposition method, the compounding technique, has been used to obtain relatively accurate approximations. The technique consists of reducing a complicated problem into a number of simpler configurations with known solutions. By superposition of these simpler K solutions, a stress intensity factor may be obtained for the complicated geometry. In equation form,

$$K_{\text{tot}} = K_0 + \left[\sum_{n=1}^{N} (K_n - K_0)\right] + K_e \tag{3.3}$$

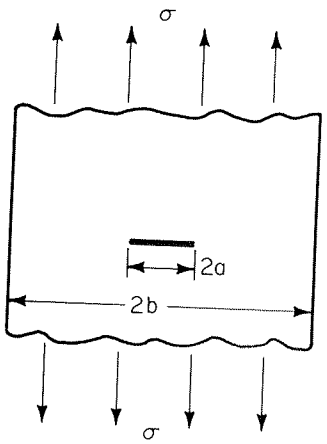

$K_I = f(g)\sigma\sqrt{\pi a}$

$f(g) = \sqrt{\sec\left(\frac{\pi a}{2b}\right)}$

(a)

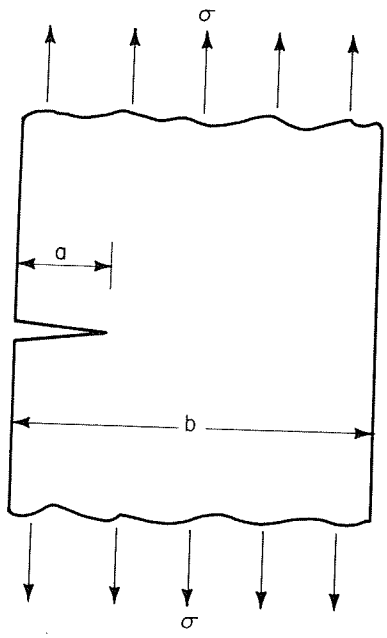

$K_I = f(g)\sigma\sqrt{\pi a}$

$f(g) = 1.12 - 0.231(a/b) + 10.55(a/b)^2 - 21.72(a/b)^3 + 30.39(a/b)^4$

(b)

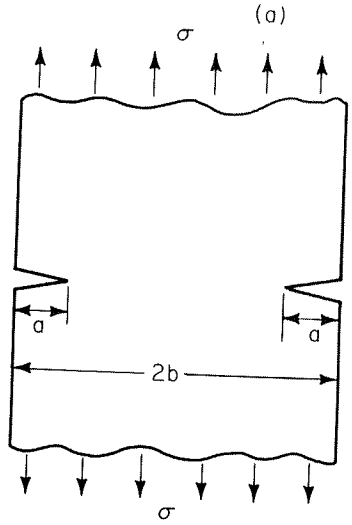

$K_I = f(g)\sigma\sqrt{\pi a}$

$f(g) = 1.12 + 0.203(a/b) - 1.197(a/b)^2 + 1.930(a/b)^3$

(c)

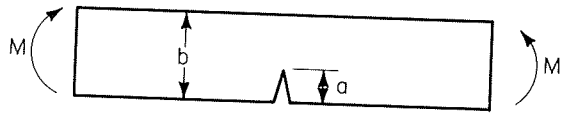

t = Thickness

$\sigma = 6M/tb^2$

$K_I = f(g)\sigma\sqrt{\pi a}$

$f(g) = 1.122 - 1.40(a/b) + 7.33(a/b)^2 - 13.08(a/b)^3 + 14.0(a/b)^4$

(d)

Figure 3.4 Stress intensity factor for (a) Center-cracked plate loaded in tension (from Ref. 10), (b) Edge-cracked plate loaded in tension (from Ref. 11), (c) Double-edge-cracked plate loaded in tension (from Ref. 12), (d) Cracked beam in pure bending (from Ref. 12), (e) Circular (penny shaped) crack embedded in infinite body subjected to tension (from Ref. 13), (f) Elliptical crack embedded in infinite body subjected to tension (from Ref. 14–15).

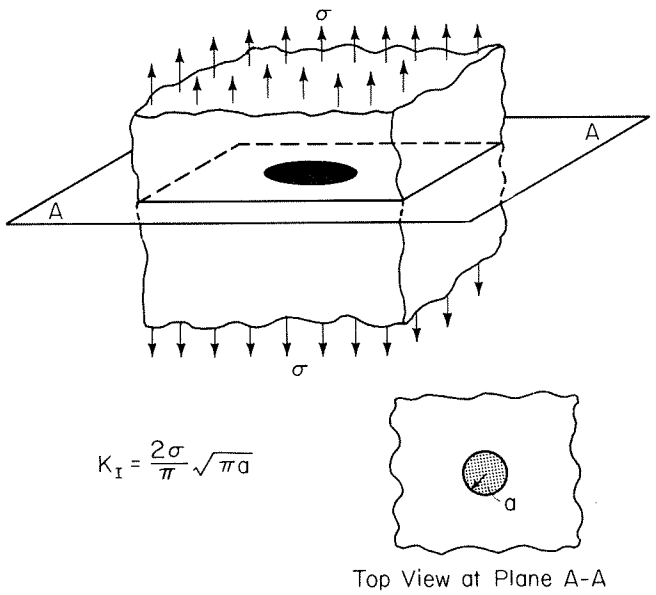

(e)

Figure 3.4 (*Continued*)

where K_{tot} = stress intensity factor for complicated geometry
K_0 = stress intensity factor in the absence of all boundaries of a form applicable to the loading (i.e., $K_I = \sigma\sqrt{\pi a}$)
K_n = stress intensity factor for the nth simpler configuration
K_e = factor that accounts for the effect of the interaction between boundaries

K_e is the only unknown. Neglecting this term will lead to underestimates of less than 10% [16]. References 17 to 21 give more details of this approach.

Another approximate method is simply to multiply the individual correction factors for the various geometric effects, such as

$$K = f_1 \cdot f_2 \cdot f_3 \cdots \sigma\sqrt{\pi a} \tag{3.4}$$

Correction factors, f_i, are used to account for

- Finite width (back wall) effect
- Front wall effect
- Crack shape (i.e., elliptical flaw)

Other superposition methods that are employed include the alternating method and the weight function method [22–26].

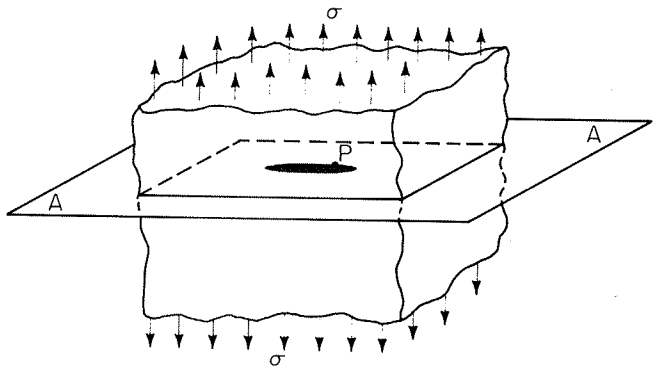

$$K_{I_{at\,P}} = \frac{\sigma\sqrt{\pi a}}{\Phi}\left\{\sin^2\theta + \frac{a^2}{c^2}\cos^2\theta\right\}^{1/4}$$

$$\Phi = \int_0^{\frac{\pi}{2}} \sqrt{1 - \left(1 - \frac{a^2}{c^2}\right)\sin^2\phi}\; d\phi$$

2c = major diameter
2a = minor diameter
Φ = Elliptical Integral

When $\theta = 90°$, K_I is Maximum
When $\theta = 0°$, K_I is Minimum

(Note: when a=b, this becomes the solution for a circular (penny shaped) crack: $K_I = \frac{2\sigma\sqrt{\pi a}}{\pi}$)

Top View at Plane A-A

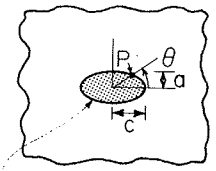

$$\frac{x^2}{c^2} + \frac{y^2}{a^2} = 1 \quad (c > a)$$

The value for the elliptical integral, Φ, for a number of a/c values is:

a/c	0	0.1	0.2	0.3	0.4	0.5	0.6	0.7	0.8	0.9	1.0
Φ	1.000	1.016	1.051	1.097	1.151	1.211	1.277	1.345	1.418	1.493	1.571

(f)

Figure 3.4 (*Continued*)

In determining K, numerical methods (including finite element methods) have been widely used in recent years. In fact, many commercially available finite element computer programs include subroutines to calculate K. References 27 to 33 review numerical techniques used to determine K.

Determination methods for K tend to be approximate. In general, values for $f(g)$ in Eq. (3.2) tend to be between 1 and 1.4, with the value for many engineering situations being between 1 and 1.2. Errors in K may be small compared to uncertainties in a fatigue analysis, such as material properties, load levels, load history, and service environment.

Example 3.1

As discussed in this section, an approximate method to obtain the stress intensity factor for a complicated geometry is simply to approximate the geometric correction factor by the product of the individual correction factors for the various geometric effects.

For the semi-elliptical surface crack in a finite thickness plate subjected to Mode I loading:

$$K_I = f_1 f_2 \cdots f_n \frac{\sigma\sqrt{\pi a}}{\Phi}\left(\sin^2\theta + \frac{a^2}{c^2}\cos^2\theta\right)^{1/4}$$

where $f_1, f_2, \ldots, f_n$ are the individual correction factors for the various geometric effects.

Using this method, determine an estimate for the stress intensity factor for a semi-circular crack in a thick plate (see Fig. E3.1a). Also using this method, estimate the stress intensity factor, K_I, for the circular corner crack in the plate shown in Fig. E3.1b.

Solution For the stress intensity factor for a semi-circular crack in a thick plate,

$$K_I \approx 1.12\left(\frac{2\sigma\sqrt{\pi a}}{\pi}\right)$$

where $f_1 = 1.12$ is the free edge correction factor and $2\sigma\sqrt{\pi a}/\pi$ is the stress intensity for a circular crack embedded in an infinite body subjected to tension (see Fig.

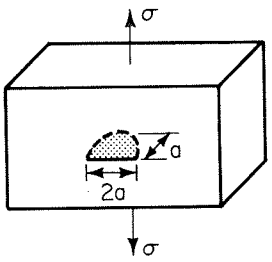

$K_I \doteq 1.12\ (\frac{2\sigma\sqrt{\pi a}}{\pi})$

(a) Semi-Circular Crack in Thick Plate

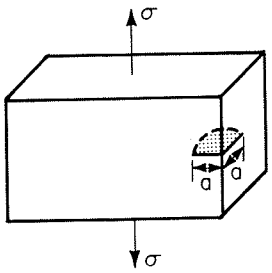

$K_I \doteq (1.12)^2\,(\frac{2\sigma\sqrt{\pi a}}{\pi})$

(b) Circular Corner Crack in Thick Plate

Figure E3.1 Stress intensity factors for: (a) a semi-circular crack in a thick plate; (b) a circular corner crack in a thick plate.

3.4e). The stress intensity factor for a circular corner crack in a thick plate

$$K_I \approx (1.12)^2(2\sigma)\frac{\sqrt{\pi a}}{\pi}$$

where $f_1 = 1.12$, the free edge correction factor for one face of the plate
$f_2 = 1.12$, the free edge correction factor the other face of the plate
$\frac{2\sigma\sqrt{\pi a}}{\pi}$ = Mode I stress intensity factor for a circular crack embedded in an infinite body subjected to tension

3.2.5 Plastic Zone Size

As mentioned previously, materials develop plastic strains as the yield stress is exceeded in the region near the crack tip (see Fig. 3.5). The amount of plastic deformation is restricted by the surrounding material, which remains elastic. The size of this plastic zone is dependent on the stress conditions of the body.

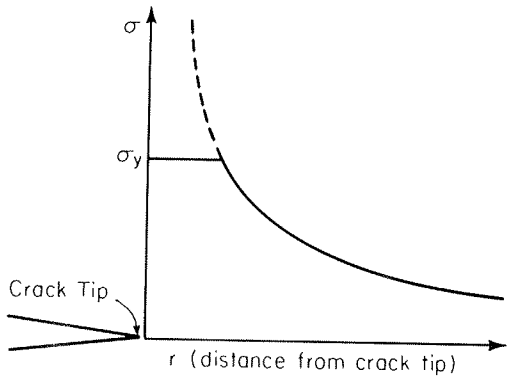

Figure 3.5 Yielding near crack tip.

Plane stress and plane strain conditions. In a thin body, the stress through the thickness (σ_z) cannot vary appreciably due to the thin section. Because there can be no stresses normal to a free surface, $\sigma_z = 0$ throughout the section and a biaxial state of stress results. This is termed a *plane stress condition* (see Fig. 3.6).

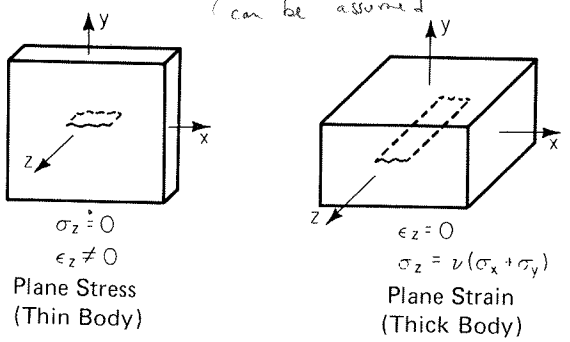

Figure 3.6 Plane stress and plane strain conditions.

In a thick body, the material is constrained in the z direction due to the thickness of the cross section and $\epsilon_z = 0$, resulting in a *plane strain condition.* Due to Poisson's effect, a stress, σ_z, is developed in the z direction. Maximum constraint conditions exist in the plane strain condition, and consequently the plastic zone size is smaller than that developed under plane stress conditions.

Monotonic plastic zone size. The plastic zone sizes under monotonic loading have been estimated to be

$$r_y = \begin{cases} \dfrac{1}{2\pi}\left(\dfrac{K}{\sigma_y}\right)^2 & \text{plane stress} \quad (3.5a) \\ \dfrac{1}{6\pi}\left(\dfrac{K}{\sigma_y}\right)^2 & \text{plane strain} \quad (3.5b) \end{cases}$$

where r is defined as shown in Fig. 3.7.

Cyclic plastic zone size. The reversed or cyclic plastic zone size is four times smaller than the comparable monotonic value. As the nominal tensile load is reduced, the plastic region near the crack tip is put into compression by the surrounding elastic body. As shown in Fig. 3.8, the change in stress at the crack tip due to the reversed loading is twice the value of the yield stress.

Equations (3.5a) and (3.5b) become

$$r_y = \begin{cases} \dfrac{1}{2\pi}\left(\dfrac{K}{2\sigma_y}\right)^2 = \dfrac{1}{8\pi}\left(\dfrac{K}{\sigma_y}\right)^2 & \text{plane stress} \quad (3.6a) \\ \dfrac{1}{6\pi}\left(\dfrac{K}{2\sigma_y}\right)^2 = \dfrac{1}{24\pi}\left(\dfrac{K}{\sigma_y}\right)^2 & \text{plane strain} \quad (3.6b) \end{cases}$$

The cyclic plastic zone size is smaller than the monotonic and more characteristic of a plane strain state even in thin plates. Thus LEFM concepts can

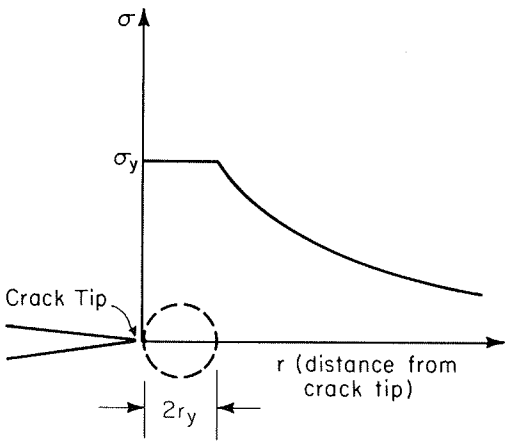

Figure 3.7 Monotonic plastic zone size.

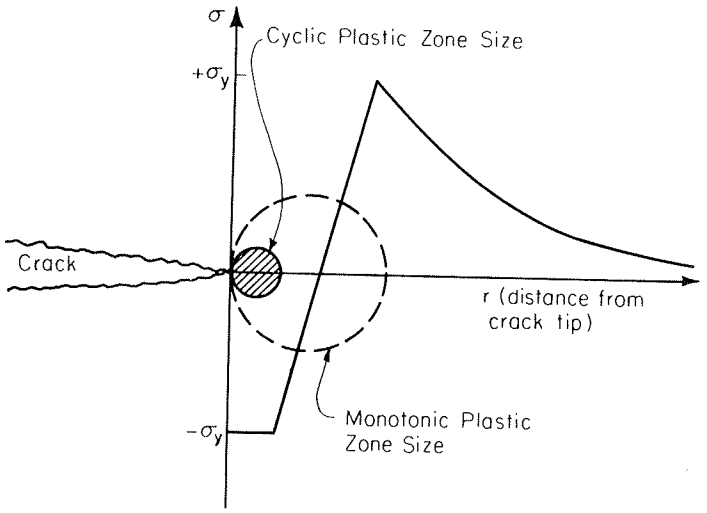

Figure 3.8 Reversed plastic zone size.

often be used in the analysis of fatigue crack growth problems even in materials that exhibit considerable amounts of ductility. The basic assumption that the plastic zone size is small in relationship to the crack and the cracked body usually remains valid.

3.2.6 Fracture Toughness

As the stress intensity factor reaches a critical value, K_c, unstable fracture occurs. This critical value of the stress intensity factor is known as the fracture toughness of the material. The fracture toughness can be considered the limiting value of stress intensity just as the yield stress might be considered the limiting value of applied stress.

The fracture toughness varies with specimen thickness until limiting conditions (maximum constraint) are reached. Recall that maximum constraint conditions occur in the plane strain state. The plane strain fracture toughness, K_{Ic}, is dependent on specimen geometry and metallurgical factors. ASTM Designation E-399, Standard Method of Test for Plane Strain Fracture Toughness of Metallic Materials, sets forth accepted procedures for determining this value. It is often difficult to perform a valid test for K_{Ic}. For example, a valid test using a thin plate of high toughness material often cannot be performed. Rather the value, K_c, at the given conditions is obtained.

The fracture toughness depends on both temperature and the specimen thickness. The following example shows the importance of the fracture toughness in designing against unstable fracture. (Also see the problems at the end of the chapter.)

Example 3.2

A company is building a 3 ft diameter pressure vessel from material that has a fracture toughness of 60 ksi $\sqrt{\text{in.}}$ and a yield strength of 85 ksi at the operating temperature. The wall thickness is 0.75 in., and the operating pressure is 2000 psi.

It is required that the vessel "leak-before-burst." In other words, the crack must be able to grow through the wall thickness before fast fracture occurs. This allows the gas or liquid in the pressure vessel to escape and be detected before an unstable condition develops.

The pressure vessel will be inspected periodically with a technique that can reliably detect a crack with a surface length larger than 0.5 in. Will the pressure vessel leak before burst when the surface length of the crack is smaller than this size? What is the largest value of the surface crack that can develop and still maintain the leak-before-burst criteria?

Solution The stress intensity for a thumbnail crack in a plate subjected to tension can be calculated from the equations in Fig. 3.4f and a free surface correction of 1.12. The stress intensity for $\theta = \pi/2$ is

$$K_I = \frac{1}{\sqrt{Q}} 1.12\sigma\sqrt{\pi a}$$

where Q is termed the shape factor since it depends on a and c. Figure E3.2 graphically shows this dependence for various ratios of nominal applied stress, σ, to the yield stress, σ_y.

Using this figure, the leak-before-burst problem can be evaluated. The following information is known:

$$K_{Ic} = 60 \text{ ksi } \sqrt{\text{in.}}$$
$$\sigma_y = 85 \text{ ksi}$$
$$p = 2000 \text{ psi}$$
$$r = d/2 = 3 \text{ ft}/2 = 18 \text{ in.}$$
$$t = 0.75 \text{ in.}$$

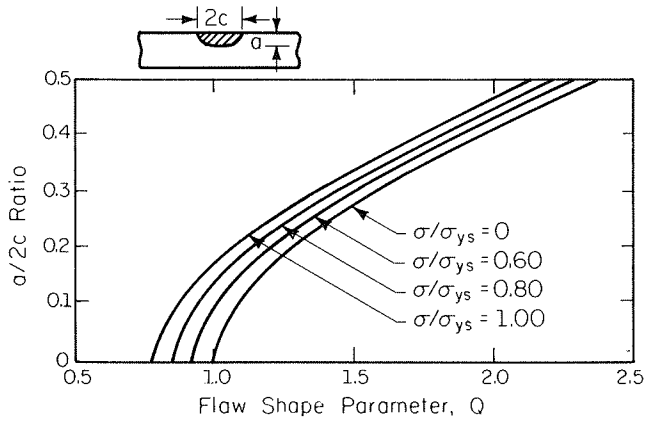

Figure E3.2 Flaw shape parameter as a function of crack aspect ratio. (From Ref. 34.)

The hoop stress in the pressure vessel is

$$\sigma = \frac{pr}{t} = 2000 \text{ psi}\left(\frac{18 \text{ in.}}{0.75 \text{ in.}}\right) = 48.0 \text{ ksi}$$

and the ratio of this stress to the yield stress is

$$\frac{\sigma}{\sigma_y} = \frac{48}{85} = 0.56$$

For the leak-before-burst criteria the critical stress intensity factor, K_{Ic}, must be larger than the stress intensity factor due to a 0.75-in. crack in the pressure vessel ($a = 0.75$ in., the wall thickness). From this information, the value for the shape factor, Q, can be determined.

$$K_{Ic} > \frac{\sigma\sqrt{\pi a}}{\sqrt{Q}}(1.12)$$

$$60 > \frac{48\sqrt{\pi(0.75)}}{\sqrt{Q}}(1.12)$$

$$Q > 1.892$$

Using Fig. E3.2, for a value of $Q > 1.892$ and $\sigma/\sigma_y = 0.56$, the value of c, the surface crack length, can now be determined:

$$\frac{a}{2c} > 0.40$$

or

$$\frac{0.75}{2(0.40)} > c$$

Therefore,

$$c < 0.938$$

and

$$2c < 1.875 \text{ in.}$$

A surface crack of 1.875 in. length or smaller will ensure that the vessel will leak before break. Thus the vessel will not fail catastrophically when a surface crack of 0.5 in. can be detected.

3.3 FATIGUE CRACK GROWTH

As discussed earlier, the majority of fatigue life may be taken up in the propagation of a crack. By the use of fracture mechanics principles it is possible

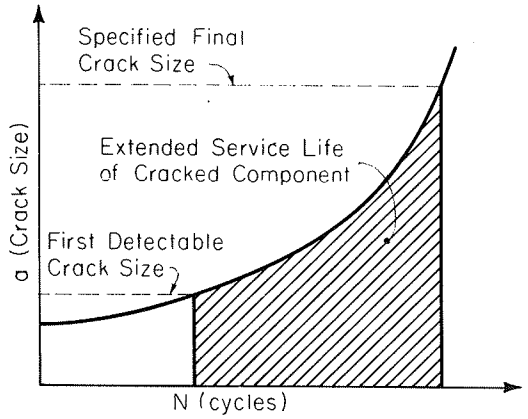

Figure 3.9 Extended service life of a cracked component.

to predict the number of cycles spent in growing a crack to some specified length or to final failure.

The aircraft industry has been instrumental in the effort to understand and predict fatigue crack growth. They have developed the safe-life or fail-safe design approach. In this method, a component is designed such that if a crack forms, it will not grow to a critical size between specified inspection intervals. Thus, by knowing the material growth rate characteristics and with regular inspections, a cracked component may be kept in service for an extended useful life. This concept is shown schematically in Fig. 3.9.

3.3.1 Fatigue Crack Growth Curves

Typical constant amplitude crack propagation data are shown in Fig. 3.10. The crack length, a, is plotted versus the corresponding number of cycles, N, at which the crack was measured. As shown, most of the life of the component is spent while the crack length is relatively small. In addition, the crack growth rate increases with increased applied stress.

The crack growth rate, da/dN, is obtained by taking the derivative of the above crack length, a, versus cycles, N, curve. (Two generally accepted numerical approaches for obtaining this derivative are the spline fitting method and the incremental polynomial method. These methods are explained in detail in many numerical methods textbooks. For example, see Ref. 35.) Values of $\log da/dN$ can then be plotted versus $\log \Delta K$, for a given crack length, using the equation

$$\Delta K = K_{\max} - K_{\min} = f(g)\,\Delta\sigma\sqrt{\pi a} \tag{3.7}$$

where $\Delta\sigma$ is the remote stress applied to the component as shown in Fig. 3.11.

A plot of $\log da/dN$ versus $\log \Delta K$, a sigmoidal curve, is shown in Fig. 3.12. This curve may be divided into three regions. At low stress intensities, Region I, cracking behavior is associated with threshold, ΔK_{th}, effects. In the mid-region,

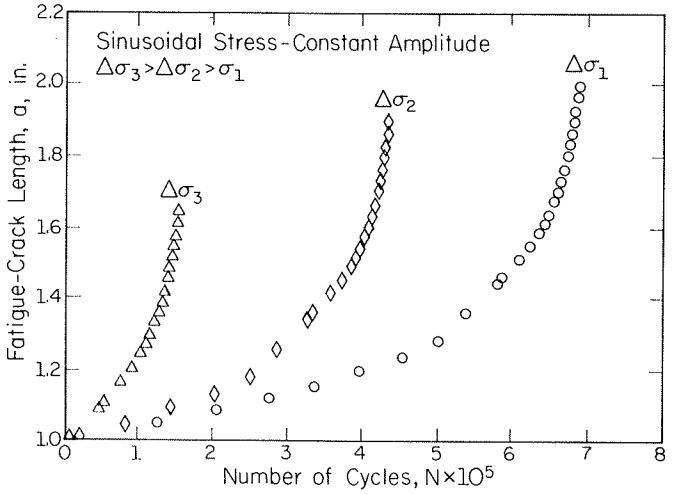

Figure 3.10 Constant amplitude crack growth data. (From Ref. 34.)

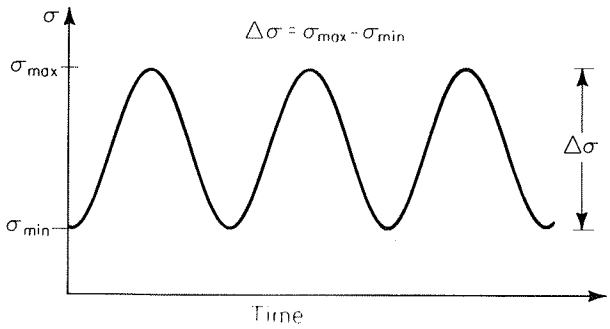

Figure 3.11 Remote stress range.

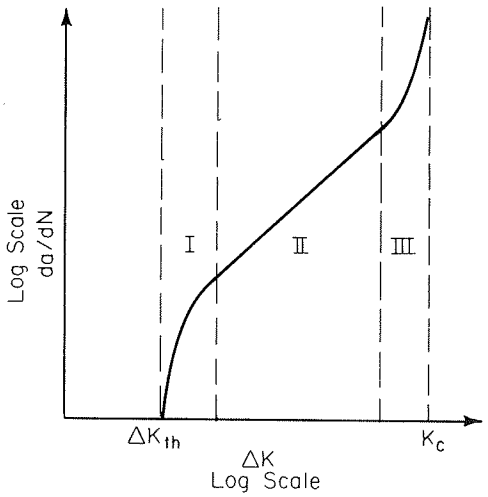

Figure 3.12 Three regions of crack growth rate curve.

Region II, the curve is essentially linear. Many structures operate in this region. Finally, in Region III, at high ΔK values, crack growth rates are extremely high and little fatigue life is involved. These three regions are discussed in detail in the following sections.

3.3.2 Region II

Most of the current applications of LEFM concepts to describe crack growth behavior are associated with Region II. In this region the slope of the $\log da/dN$ versus $\log \Delta K$ curve is approximately linear and lies roughly between 10^{-6} and 10^{-3} in./cycle. Many curve fits to this region have been suggested. The Paris [36] equation, which was proposed in the early 1960s, is the most widely accepted. In this equation

$$\frac{da}{dN} = C(\Delta K)^m \tag{3.8}$$

where C and m are material constants and ΔK is the stress intensity range $K_{max} - K_{min}$.

The material constants, C and m, can be found in the literature and in data books such as Refs. 34 and 37. Values of the exponent, m, are usually between 3 and 4. Reference 38 tabulates values of m for a number of metals. These range from 2.3 to 6.7 with a sample average of $m = 3.5$. In addition, tests may be performed. ASTM E647 sets guidelines for these tests.

The crack growth life, in terms of cycles to failure, may be calculated using Eq. (3.8). The relation may be generally described by

$$\frac{da}{dN} = f(K)$$

Thus, cycles to failure, N_f, may be calculated as

$$N_f = \int_{a_i}^{a_f} \frac{da}{f(K)} \tag{3.9}$$

where a_i is the initial crack length and a_f is the final (critical) crack length. Using the Paris formulation,

$$\frac{da}{dN} = C(\Delta K)^m$$

$$N_f = \int_{a_i}^{a_f} \frac{da}{C(\Delta K)^m} \tag{3.10}$$

Because ΔK is a function of the crack length and a correction factor that is dependent on crack length [see Eq. (3.7)], the integration above must often be solved numerically. As a first approximation, the correction factor, $f(g)$, can be

s range.

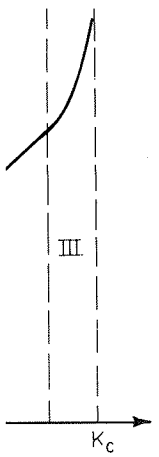

calculated at the initial crack length and Eq. (3.10) can be evaluated in closed form.

As an example of a closed form integration, fatigue life calculations for a small edge-crack in a large plate are performed below. In this case the correction factor, $f(g)$, does not vary with crack length. The stress intensity factor range is

$$\Delta K = 1.12\Delta\sigma\sqrt{\pi a} \tag{3.11}$$

Substituting into the Paris equation yields

$$\frac{da}{dN} = C(1.12\Delta\sigma\sqrt{\pi a})^m \tag{3.12}$$

Separating variables and integrating (for $m \neq 2$) gives

$$N_f = \int_{a_i}^{a_f} \frac{da}{C(1.12\Delta\sigma\sqrt{\pi a})^m}$$

$$= \frac{2}{(m-2)C(1.12\Delta\sigma\sqrt{\pi})^m}\left(\frac{1}{a_i^{(m-2)/2}} - \frac{1}{a_f^{(m-2)/2}}\right) \tag{3.13}$$

Before this equation may be solved, the final crack size, a_f, must be evaluated. This may be done using Eq. (3.2) as follows:

$$K = f(g)\sigma\sqrt{\pi a}$$

$$a_f = \frac{1}{\pi}\left[\frac{K_c}{\sigma f(g)}\right]^2 \tag{3.14}$$

$$= \frac{1}{\pi}\left(\frac{K_c}{1.12\sigma_{\max}}\right)^2 \tag{3.15}$$

For more complicated formulations of ΔK, where the correction factor varies with the crack length, a, iterative procedures may be required to solve for a_f in Eq. (3.14).

It is important to note that the fatigue-life estimation is strongly dependent on a_i, and generally not sensitive to a_f (when $a_i \ll a_f$). Large changes in a_f result in small changes of N_f, as shown schematically in Fig. 3.13.

An alternative approximate method may be used to predict fatigue crack growth under constant-amplitude loading. This procedure is outlined in Ref. 39 and discussed in Refs. 6 and 16. Briefly, the procedure is as follows:

1. Divide the interval of crack growth from a_i to a_f into a desired number of increments, $n - 1$.
2. In Eq. (3.7), determine $f(g)$ for each of the intermediate crack lengths as well as the initial and final lengths, a_i and a_f, respectively.
3. Calculate a ΔK_n for each crack length, a_n.

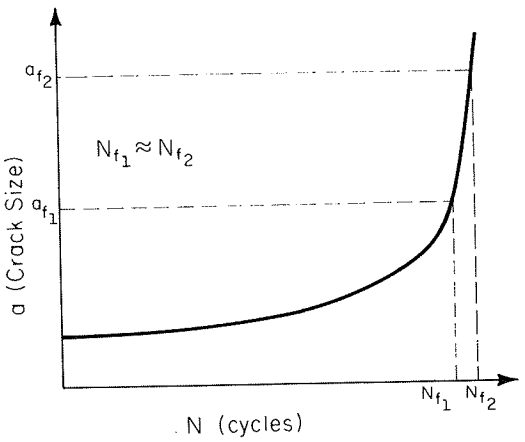

Figure 3.13 Effect of final crack size on life.

4. For each ΔK_n, determine the corresponding da/dN from crack growth rate plots or the Paris equation:

$$\left(\frac{da}{dN}\right)_n = C(\Delta K_n)^m \tag{3.16}$$

5. Average the growth rates for two consecutive crack lengths:

$$\frac{(da/dN)_n + (da/dN)_{n+1}}{2} = \left(\frac{da}{dN}\right)_{\text{average}} \tag{3.17}$$

6. Determine the number of cycles for the growth during the crack increment, a_n to a_{n+1}, by

$$\Delta N = \frac{\Delta a}{(da/dN)_{\text{average}}} = \frac{2(a_{n+1} - a_n)}{(da/dN)_n + (da/dN)_{n+1}} \tag{3.18}$$

Thus an approximate value is obtained for the number of cycles for an increment of crack growth. These values of ΔN for each increment may then be summed for an approximate solution for the number of loading cycles for the growth of the crack between the two lengths, a_i and a_f.

Usually the fatigue life is not sensitive to the fracture toughness of the material. This is a result of the lack of sensitivity of N_f to the final crack size, a_f, as shown in Fig. 3.13. An exception to this would be a case where a very hard material is subjected to large stresses. For instance, the fatigue life of gears is dependent on the fracture toughness of the material because the initial crack size varies little from the final crack length.

3.3.3 Region I

Region I of the sigmoidal crack growth rate curve is associated with threshold effects. Below the value of the threshold stress intensity factor, ΔK_{th}, fatigue

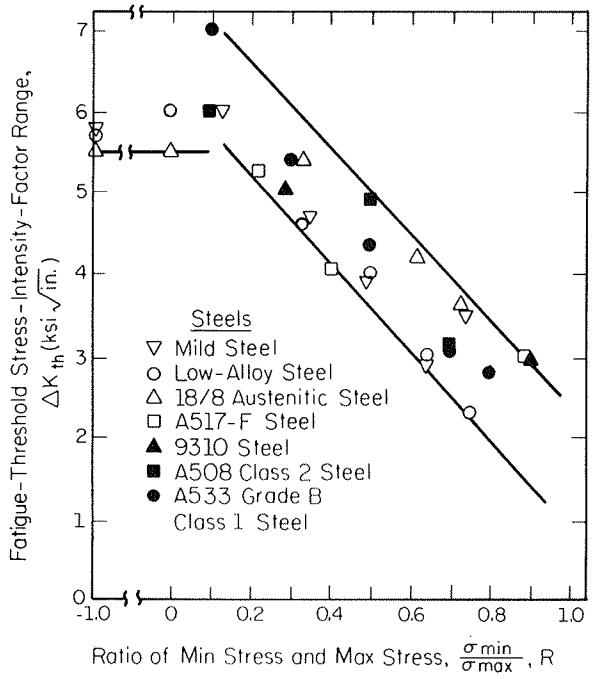

Figure 3.14 Dependence of fatigue-threshold stress-intensity-factor range on stress ratio. (From Ref. 34.)

crack growth does not occur or occurs at a rate too slow to measure. (The smallest measured rates are larger than approximately 10^{-8} in./cycle. This corresponds to the spacing between atoms in most metals.)

The fatigue threshold for steels is usually between 5 and 15 ksi $\sqrt{\text{in.}}$ and between 3 and 6 ksi $\sqrt{\text{in.}}$ for aluminum alloys. The fatigue threshold is dependent on the stress ratio, R ($R = \sigma_{min}/\sigma_{max}$). As seen in Fig. 3.14, the fatigue threshold decreases with increasing stress ratio.

The threshold also depends on frequency of loading and environment (see Section 3.3.5). In addition, many of the published threshold values, ΔK_{th}, were developed for long cracks. The validity of these values for short cracks has recently been questioned. In Ref. 40 an empirical relationship between the ΔK_{th} for short cracks and the ΔK_{th} for long cracks has been proposed. Several methods for measuring ΔK_{th} are reviewed in Ref. 28. In fact, due to the sensitivity of ΔK_{th} to environment and load history, it is felt by many that the best method for determining ΔK_{th} is through testing under conditions that simulate actual service conditions. References 37 and 41 to 43 give more detailed information on fatigue threshold concepts, testing, and results.

Designing a component such that ΔK for service conditions would be below ΔK_{th} would be highly desirable. Although this would ensure a low probability of fatigue failure, this is often impractical due to the low level of operating stress required. Alternatively, ensuring that defects were so small that the ΔK was

below the threshold would be equally desirable. Unfortunately, the defect size required is not only impractical but unattainable.

For example, given below are typical values for the endurance limit and fatigue threshold for a common steel. Calculations to determine the maximum defect size in an infinite plate with a center crack are outlined.

$$S_e \approx 50 \text{ ksi}$$

$$\Delta K_{th} = 5 \text{ ksi} \sqrt{\text{in.}}$$

$$K = \sigma\sqrt{\pi a}$$

$$f(g) = 1 \quad \text{(for an infinite center-cracked plate)}$$

From Eq. (3.14), the critical crack size is calculated:

$$a_c = \frac{1}{\pi}\left[\frac{1}{f(g)}\left(\frac{K_c}{\sigma_{max}}\right)\right]^2 \tag{3.19}$$

$$= \frac{1}{\pi}\left(\frac{5}{50}\right)^2$$

$$= 0.003 \text{ in.}$$

This defect size is on the order of that obtained due to normal fabrication or machining of a component. Thus, even at the endurance limit, which is a relatively low stress, the defect size is one that would be extremely difficult to detect using nondestructive inspection methods.

The threshold value may be of use when a part is subjected to low stress levels and a very large number of cycles. A good example of this would be power trains that operate at very high speeds.

3.3.4 Region III

In Region III, rapid, unstable crack growth occurs. In many practical engineering situations this region may be ignored because it does not significantly affect the total crack propagation life.

The point of transition from Region II to Region III behavior is dependent on the yield strength of the material, stress intensity factor, and stress ratio. Forman's equation [44] was developed to model Region III behavior, although it is more often used to model mean stress effects. This equation,

$$\frac{da}{dN} = \frac{C\,\Delta K^m}{(1 - R)K_c - \Delta K} \tag{3.20}$$

predicts the sharp upturn in the da/dN versus ΔK curve as fracture toughness is approached. (This equation is discussed further in Section 3.3.5).

Region III is of most interest when the crack propagation life is on the order of 10^3 cycles or less. At high stress intensities, though, the effects of plasticity

start to influence the crack growth rate because the plastic zone size becomes large compared to the dimensions of the crack. In this case, the problem should be analyzed by some elastic–plastic fracture approach such as the J-integral or the crack-tip opening displacement (COD) methods.

3.3.5 Factors Influencing Fatigue Crack Growth

Stress ratio effects. The applied stress ratio, R, can have a significant effect on the crack growth rate. Recall, as defined in Section 3.3.3, $R = \sigma_{min}/\sigma_{max} = K_{min}/K_{max}$. In general, for a constant ΔK, the more positive the stress ratio, R, the higher the crack growth rates, as shown in Fig. 3.15. The stress ratio sensitivity, though, is strongly dependent on material as shown in Figs. 3.15 and 3.16. (Note the difference of the scales on the two figures.)

Forman's equation [Eq. (3.20)] is often used to predict stress ratio effects. As R increases, the crack growth rate, da/dN, increases. This is consistent with test observations. Forman's equation is valid only when $R > 0$. Generally, it is believed that when $R < 0$, no significant change in growth rate occurs compared to the $R = 0$ growth rate. Again this is material dependent, as some researchers have obtained data for certain materials which show higher growth rates for $R < 0$ loading [45, 46].

Another method used to compensate for stress ratio effects is *Walker's equation* [47]:

$$\frac{da}{dN} = C[(1 - R)^m K_{max}]^n \tag{3.21}$$

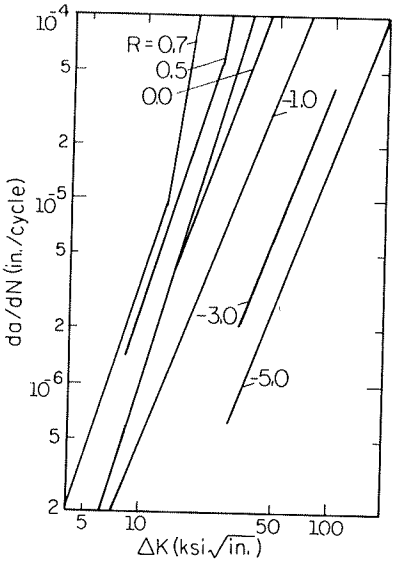

Figure 3.15 Influence of R on fatigue crack growth in Ti–6Al–4V. (From Ref. 48.)

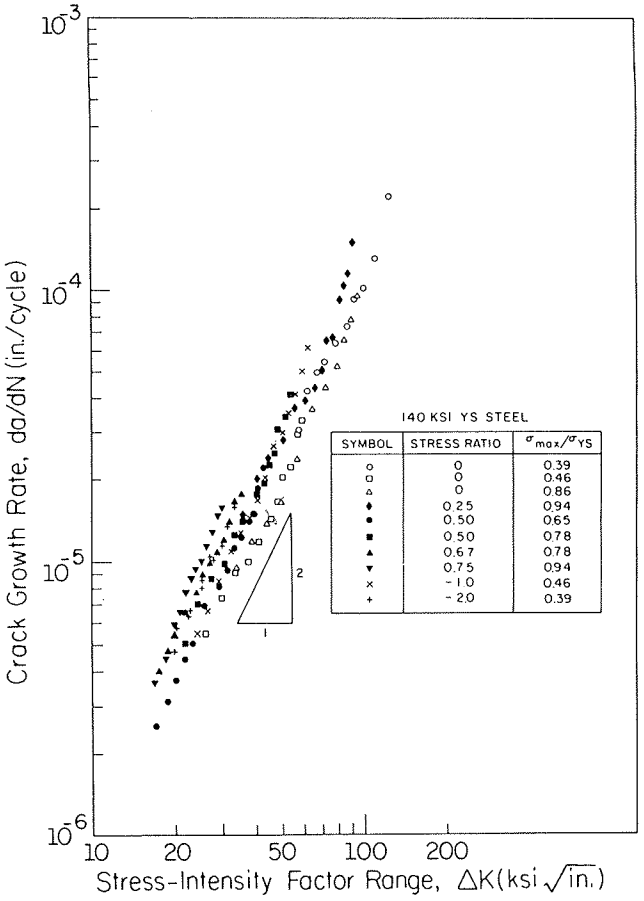

Figure 3.16 No major influence of R on fatigue crack growth in 140-ksi yield strength steel. (From Ref. 49.)

Use of this equation requires that stress ratio data be available to fit the exponents m and n for a particular material.

Crack closure arguments, as well as arguments based on environmental effects, have been used to explain the stress ratio effect on crack growth rates. Both of these topics are discussed in further detail in later sections.

Environmental effects. The fatigue crack growth rate can be greatly influenced by environmental effects. These effects are extremely complicated due to the large number of mechanical, metallurgical, and chemical variables and the interaction between them. Because of this complexity, only an overview is presented here. A more detailed discussion is found in Ref. 50 with a comprehensive literature review presented in Ref. 28.

The environmental effect on fatigue crack growth rate is strongly dependent on the material–environment combination. Several additional factors that in-

fluence the environmental effect are the following:

Frequency of loading. In an adverse environment, a strong effect of cyclic loading frequency is observed. No frequency effect is observed on the fatigue crack growth rate for a material tested in an inert environment. In general, at low frequencies, crack growth rates increase as more time is allowed for environmental attack during the fatigue process.

Temperature effects. Reduced fatigue life is usually observed with increasing temperature. In addition, environmental effects are usually greater at

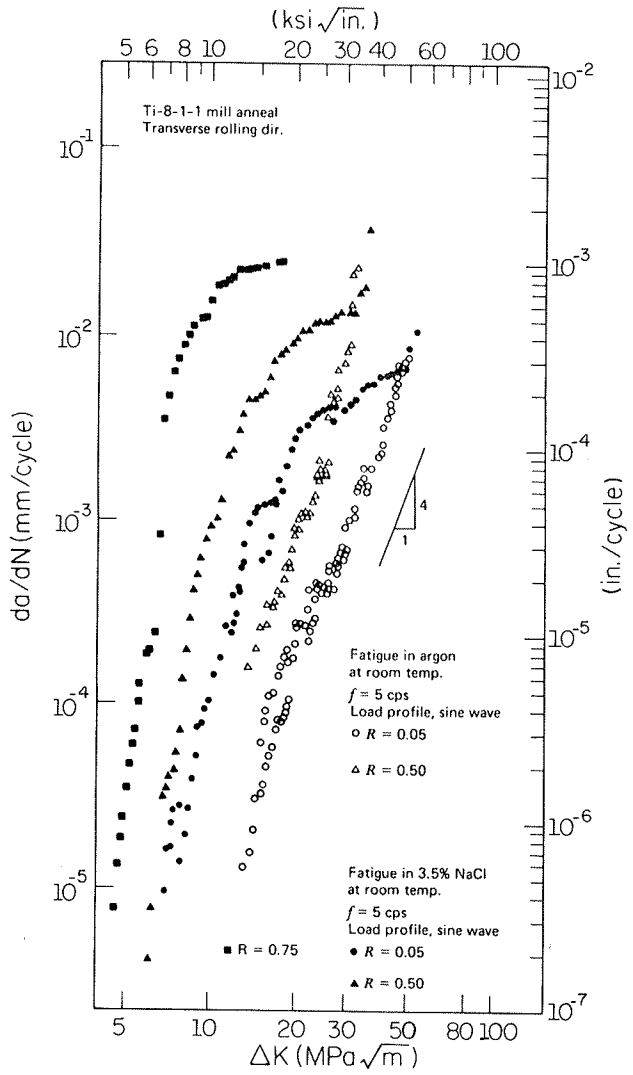

Figure 3.17 Effect of load ratio R on fatigue crack propagation in Ti–8Al–1Mo–1V alloy. Tests conducted in 3.5% NaCl solution and in argon. (From Ref. 51.)

elevated temperatures. This is due in part to oxide growth, which both promotes intergranular cracking and accelerates transgranular cracking.

Waveform of loading cycle. Higher fatigue crack growth rates generally occur if the increasing (tensile) portion of the loading cycle occurs more slowly. In other words, when the load rise time is small, the environmental influence is minimized. For example, a positive sawtooth waveform, /\/\, results in a higher environmental effect and consequently, increased crack growth rate than a negative sawtooth waveform, \/\/. No effect of waveform profile is usually observed in air.

Stress ratio effects. As discussed previously, some researchers feel that environmental effects may cause fatigue crack growth rate sensitivity to stress ratio, R, effects. At high R ratios, enhanced corrosion occurs, as demonstrated in Fig. 3.17.

Finally, environmental effects have been observed to cause either an increase or a decrease in ΔK_{th}, depending on material and environment. The increase in ΔK_{th} may be explained in some situations by local corrosion or oxides on the crack surfaces. These oxides increase the volume of material, contributing to the crack closure effect. The principles of crack closure are discussed below.

3.3.6 Crack Closure

Crack closure arguments are often used to explain the stress ratio effect of crack growth rates as well as environmental effects on ΔK_{th}. In addition, crack closure theories are very important in variable amplitude fatigue crack growth predictions, which are discussed in Chapter 5.

In the early 1970s, Elber [52] observed that the surfaces of fatigue cracks close (contact each other) when the remotely applied load is still tensile and do not open again until a sufficiently high tensile load is obtained on the next loading cycle. He developed the theory of crack closure to explain this phenomenon.

Elber proposed that crack closure occurs as a result of crack-tip plasticity. Recall from Section 3.2.5 that a plastic zone develops around the crack tip as the yield stress of the material is exceeded. As shown in Fig. 3.18, as the crack grows, a wake of plastically deformed material is developed while the surrounding body

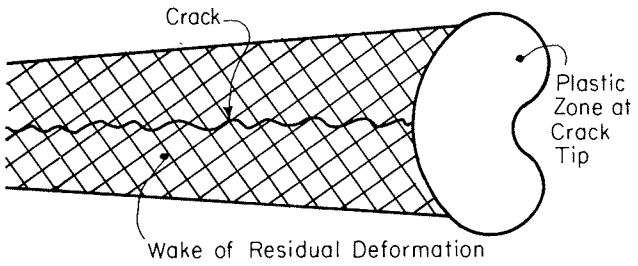

Figure 3.18 Wake of plastically deformed material.

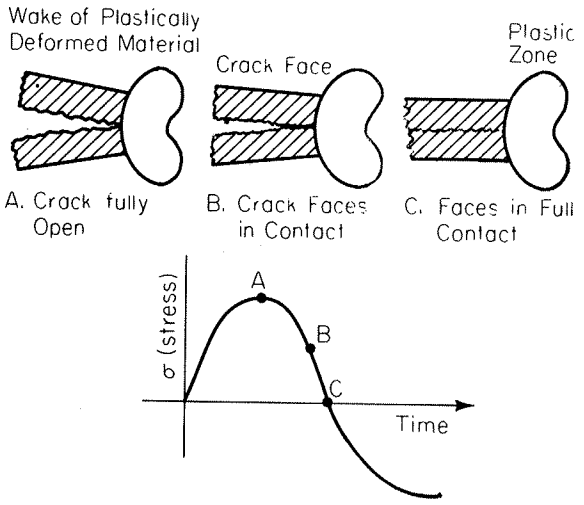

Figure 3.19 Crack closure phenomenon.

remains elastic. (Figure 3.18 shows the case of a gradually increasing ΔK and consequently, gradually increasing plastic zone size.) Elber proposed that as the component is unloaded, the plastically "stretched" material causes the crack surfaces to contact each other before zero load is reached (see Fig. 3.19).

Elber further introduced the idea of a crack-opening stress. This is the value of applied stress at which the crack is just fully open, σ_{op}. He suggested that for fatigue crack growth to occur, the crack must be fully open:

$$\begin{aligned} \Delta K_{eff} &= K_{max} - K_{open} \\ \Delta K &= K_{max} - K_{min} \end{aligned} \tag{3.22}$$

since

$$K_{open} > K_{min}$$

Consequently,

$$\Delta K > \Delta K_{eff}$$

Therefore, an effective stress intensity factor range, ΔK_{eff}, which is smaller than ΔK, should be used in fatigue crack growth predictions.

$$\frac{da}{dN} = f(\Delta K_{eff}) \tag{3.23}$$

Elber proposed that ΔK_{eff} accounts for the R effect on growth rates. At higher values of R, less crack closure results and ΔK_{eff} becomes closer to ΔK because K_{open} approaches K_{min}. This results in the crack being subjected to a

greater range of loading. He obtained the empirical relationship

$$\Delta K_{\text{eff}} = U\,\Delta K$$
$$U = \frac{\Delta K_{\text{eff}}}{\Delta K} = 0.5 + 0.4R \tag{3.24}$$

Note that Eq. (3.24) is valid only when $R > 0$. Other researchers have subsequently developed expressions for U [53] and extended these for ratios of $R < 0$.

Crack closure arguments are further discussed in connection with variable amplitude loading and crack growth retardation in Chapter 5.

3.4 IMPORTANT CONCEPTS

- Fracture mechanics approaches provide an estimate of the crack propagation fatigue life.
- In the fracture mechanics approach, the local stresses and strains are related to the remote (applied) stresses and strains by the stress intensity factor, K.
- The linear elastic fracture mechanics approach is based on the assumption that the plastic zone at the crack tip is small compared to the crack length and the size of the cracked component.
- The fatigue crack growth rate can be related to the stress intensity factor range. From this, cycles to failure may be calculated.
- The fatigue life estimate is strongly dependent on the initial crack size, a_i. Large changes in the estimate of final crack size, a_f, result in only small changes in the life estimate.

3.5 IMPORTANT EQUATIONS

Stress Intensity Factor

$$K = f(g)\sigma\sqrt{\pi a} \tag{3.2}$$

Stress Intensity Factor Range

$$\Delta K = K_{\max} - K_{\min} = f(g)\,\Delta\sigma\sqrt{\pi a} \tag{3.7}$$

Crack Growth Rate (Paris Law)

$$\frac{da}{dN} = C(\Delta K)^m \tag{3.8}$$

Cycles to Failure

$$N_f = \int_{a_i}^{a_f} \frac{da}{C(\Delta K)^m} \tag{3.10}$$

Critical (Final) Crack Size

$$a_f = \frac{1}{\pi}\left[\frac{K}{\sigma f(g)}\right]^2 \tag{3.14}$$

Effective Stress Intensity Factor Range

$$\Delta K_{\text{eff}} = K_{\max} - K_{\text{open}} \tag{3.22}$$

REFERENCES

1. A. A. Griffith, *Philos. Trans. R. Soc. London,* Vol. A221, 1920, p. 163. (This article has been republished with additional commentary in *Trans. Am. Soc. Metals,* Vol. 61, 1968, p. 871.)
2. G. R. Irwin, *Fracturing of Metals,* American Society for Metals, Cleveland, Ohio, 1949, p. 147.
3. G. R. Irwin, "Analysis of Stresses and Strains near the End of a Crack Traversing a Plate," *Trans. ASME, J. Appl. Mech.,* Vol. E24, 1957, p. 361.
4. J. F. Knott, *Fundamentals of Fracture Mechanics,* Butterworth, London, 1973.
5. D. Broek, *Elementary Engineering Fracture Mechanics,* Martinus Nijhoff, The Hague, 1982.
6. H. L. Ewalds and R. J. H. Wanhill, *Fracture Mechanics,* Edward Arnold, London, 1985.
7. H. Tada, P. C. Paris and G. R. Irwin, *The Stress Analysis of Cracks Handbook,* Del Research Corporation, Hellertown, Pa., 1973.
8. D. P. Rooke, and D. J. Cartwright, *Compendium of Stress Intensity Factors,* H.M. Stationery Office, London, 1975.
9. G. C. M. Sih, *Handbook of Stress Intensity Factors,* Lehigh University, Bethlehem, Pa., 1973.
10. C. E. Fedderson, Discussion to: "Plane Strain Crack Toughness Testing," in ASTM STP 410, American Society for Testing and Materials, Philadelphia, 1966, p. 77.
11. B. Gross and J. E. Srawley, "Stress Intensity Factors for a Single Notch Tension Specimen by Boundary Collocation of a Stress Function," NASA TN D-2395, 1964.
12. W. F. Brown and J. E. Srawley, "Plane Strain Crack Toughness Testing of High Strength Metallic Materials," in ASTM STP 410, American Society for Testing and Materials, Philadelphia, 1966.
13. I. N. Sneddon, "The Distribution of Stress in the Neighborhood of a Crack in an Elastic Solid," in *Proceedings of the Royal Society of London,* Series A, Vol. A187, 1946, p. 229.

14. M. A. Sadowsky and E. G. Sternberg, "Stress Concentration around a Triaxial Ellipsoidal Cavity," *Trans. ASME, J. Appl. Mech.*, Vol. E16, 1949, pp. 149–157.

15. A. E. Green and I. N. Sneddon, "The Distribution of Stress in the Neighborhood of a Flat Elliptical Crack in an Elastic Solid," *Proc. Cambridge Philos. Soc.*, Vol. 46, 1950, p. 159.

16. A. P. Parker, *The Mechanics of Fracture and Fatigue: An Introduction*, E. and F. N. Spon, London, 1981.

17. D. J. Cartwright and D. P. Rooke, "Approximate Stress Intensity Factors Compounded from Known Solutions," *Eng. Fract. Mech.*, Vol. 6, 1974, pp. 563–571.

18. D. P. Rooke, *Stress Intensity Factors for Cracks at the Edges of Holes*, RAE TR 76087, Royal Aircraft Establishment, Farnborough, England, 1976.

19. D. P. Rooke, "Stress Intensity Factors for Cracked Holes in the Presence of Other Boundaries," in *Fracture Mechanics in Engineering Practice*, Applied Science Publishers, Barking, Essex, England, 1977, pp. 149–163.

20. D. P. Rooke and D. J. Cartwright, "The Compounding Method Applied to Cracks in Stiffened Sheets," *Eng. Fract. Mech.*, Vol. 8, 1976, pp. 567–573.

21. *The Compounding Method of Estimating Stress Intensity Factors for Cracks in Complex Configurations Using Solutions for Simple Configurations*, Engineering Sciences Data Unit, Item No. 78036, London Royal Aeronautical Society, Nov. 1978.

22. J. R. Rice, "Some Remarks on Elastic Crack-Tip Stress Fields," *Int. J. Solids Struct.*, Vol. 8, 1972, pp. 751–758.

23. H. F. Bueckner, "A Novel Principle for the Computation of Stress Intensity Factors," *Z. Angew. Math. Mech.*, Vol. 50, 1970, p. 529.

24. P. C. Paris, R. M. McMeeking, and H. Tada, "The Weight Function Method for Determining Stress Intensity Factors," in *Cracks and Fracture*, ASTM STP 601, American Society for Testing and Materials, Philadelphia, 1976, pp. 471–489.

25. T. A. Cruse, and P. M. Besuner, "Residual Life Prediction for Surface Cracks in Complex Structural Details," *J. Aircr.*, Vol. 12, No. 4, 1975, pp. 369–375.

26. R. J. Hartranft and G. C. Sih, "Alternating Method Applied to Edge and Surface Crack Problems," in *Mechanics of Fracture I*, G. C. Sih (ed.), Sÿthoffen Noordhoff, Alphen ann den Rijn, the Netherlands, 1973, Chap. 4, pp. 179–238.

27. T. K. Hellen, "Numerical Methods in Fracture Mechanics," in *Developments in Fracture Mechanics*, Vol. 1, G. G. Chell (ed.), Applied Science Publishers, Barking, Essex, England, 1979, pp. 145–181.

28. P. M. Besuner, (ed.), *A Review of Fracture Mechanics Life Technology*, Final Report Contract NAS8-34746, prepared by Failure Analysis Associates, Palo Alto, Ca, Sept. 1983.

29. V. E. Saouma and D. Schwemmer, "Numerical Evaluation of the Quarter-Point Crack-Tip Element," *Int. J. Numer. Methods Eng.*, Vol. 20, 1984, pp. 1629–1641.

30. R. D. Henshell and K. G. Shaw, "Crack Tip Elements Are Unnecessary," *Int. J. Numer. Methods Eng.*, Vol. 9, 1975, pp. 495–507.

31. R. S. Barsoum, "On the Use of Isoparametric Elements in Linear Elastic Fracture Mechanics," *Int. J. Numer. Methods Eng.*, Vol. 10, 1976, pp. 25–37.

32. J. J. Oglesby and O. Lomacky, "An Evaluation of Finite Element Methods for the

Computation of Elastic Stress Intensity Factors," *J. Eng. Ind.*, Feb. 1973, pp. 177–184.

33. D. M. Parks, "A Stiffness Derivative Finite Element Technique for Determination of Crack Tip Stress Intensity Factors," *Int. J. Fract.*, Vol. 10, 1974, pp. 487–502.
34. S. T. Rolfe and J. M. Barsom, *Fracture and Fatigue Control in Structures*, Prentice-Hall, Englewood Cliffs, N.J., 1977.
35. S. C. Chapra and R. P. Canale, *Numerical Methods for Engineers: With Personal Computer Applications*, McGraw-Hill, New York, 1985.
36. P. C. Paris and F. Erdogan, "A Critical Analysis of Crack Propagation Laws," *Trans. ASME, J. Basic Eng.*, Vol. D85, 1963, pp. 528–534.
37. J. M. Barsom, "Fatigue-Crack Propagation in Steels of Various Yield Strengths," *Trans. ASME, J. Eng. Ind.*, Vol. B73, No. 4, Nov. 1971, p. 1190.
38. J. F. Throop, and G. A. Miller, "Optimum Fatigue Crack Resistance," in *Achievement of High Fatigue Resistance in Metals and Alloys*, ASTM STP 467, American Society for Testing and Materials, Philadelphia, 1970, p. 154.
39. Engineering Sciences Data Unit, *Examples of the Use of Data Items on Fatigue Crack Propagation Rates*, Item No. 74017, Engineering Sciences Data Unit, London Royal Aeronautical Society, 1977.
40. O. N. Romaniv, V. N. Siminkovich and A. N. Tkach, "Near Threshold Short Fatigue Crack Growth," *in Fatigue Thresholds, Fundamentals and Engineering Applications*, Vol. 2, J. Backlund, A. F. Blom, and J. C. Beevers (eds.), Engineering Materials Advisory Services Ltd., West Midlands, England, 1982, pp. 799–807.
41. J. K. Musuva and J. C. Radon, "The Effect of Stress Ratio and Frequency on Fatigue Crack Growth," *Fatigue Eng. Mater. Struct.*, Vol. 1, 1979, pp. 457–470.
42. J. Backlund, A. F. Blom and J. C. Beevers (eds.), *Fatigue Thresholds, Fundamentals and Engineering Applications*, Vols. 1 and 2, Engineering Materials Advisory Services Ltd., West Midlands, England, 1982.
43. R. A. Smith, "Fatigue Thresholds—A Design Engineer's Guide through the Jungle," in *Fatigue Thresholds, Fundamentals and Engineering Applications*, Vol. 1, J. Backlund, A. F. Blom, and J. C. Beevers (eds.), Engineering Materials Advisory Services Ltd., West Midlands, England, 1982, pp. 33–44.
44. R. G. Forman, V. E. Kearney, and R. M. Engle, "Numerical Analysis of Crack Propagation in a Cyclic-Loaded Structure," *Trans. ASME, J. Basic Eng.*, Vol. D89, No. 3, 1967, pp. 459–464.
45. C. M. Hudson, "Effect of Stress Ratio on Fatigue Crack Growth in 7075–T6 and 2024–T3 Aluminum Alloy Specimens," NASA TN–D 5390, National Aeronautics and Space Administration, Aug. 1969.
46. W. Illg, and A. J. McEvily, "The Rate of Fatigue Crack Propagation for Two Aluminum Alloys under Completely Reversed Loading," NASA TN-D-52, National Aeronautics and Space Administration, Oct. 1959.
47. K. Walker, "The Effect of Stress Ratio during Crack Propagation and Fatigue for 2024–T3 and 7075–T6 Aluminum," in *Effects of Environment and Complex Load History on Fatigue Life*, ASTM STP 462, American Society for Testing and Materials, Philadelphia, 1970, p. 1.
48. A. Yuen, S. W. Hopkins, G. R. Leverant and C. A. Rau, "Correlations between

Fracture Surface Appearance and Fracture Mechanics Parameters for Stage II Fatigue Crack Propagation in Ti-6Al-4V," *Metall. Trans.*, Vol. 5, Aug. 1974, pp. 1833–1842.

49. T. W. Crooker and D. J. Krause, "The Influence of Stress Ratio and Stress Level on Fatigue Crack Growth Rates in 140 ksi YS Steel," Report of NRL Progress, Naval Research Laboratory, Washington D.C., Dec. 1972, pp. 33–35.
50. R. W. Hertzberg, *Deformation and Fracture Mechanics of Engineering Materials,* 2nd ed., Wiley, New York, 1983.
51. R. J. Bucci, PhD. Dissertation, Lehigh University, 1970.
52. W. Elber, "The Significance of Fatigue Crack Closure," in *Damage Tolerance in Aircraft Structures,* ASTM STP 486, American Society for Testing and Materials, Philadelphia, 1971, pp. 230–242.
53. J. Schijve, *The Stress Ratio Effect on Fatigue Crack Growth in* 2024-*T*3 *Alclad and the Relation to Crack Closure,* Memorandum M-336, Delft University of Technology Department of Aerospace Engineering, Delft, the Netherlands, Aug. 1979.
54. E. M. Caufield, "Evaluation of Fracture Mechanics Parameters for A27 Cast Steel," Fracture Control Program Report No. 28, University of Illinois at Urbana–Champaign, 1977.

PROBLEMS

SECTION 3.2

3.1. A large plate made of AISI 4340 steel contains an edge crack and is subjected to a tensile stress of 40 ksi. The material has an ultimate strength of 260 ksi and a K_c value of 45 ksi $\sqrt{\text{in.}}$ Assume that the crack is much smaller than the width of the plate. Determine the critical crack size.

3.2. If the plate in Problem 3.1 is now of a finite width such that the ratio of the crack length to the plate width is 0.1, determine the critical crack size. Determine the critical crack size for a crack length to plate width ratio of 0.2.

3.3. Determine the stress intensity factor for the edge-cracked beam shown below when subjected to a moment of 400 ft-kips. If the beam was made from an extremely tough steel that has a yield strength of 195 ksi and a K_c of 160 ksi $\sqrt{\text{in.}}$ and the moment applied to the beam was increased to 1600 ft-kips, would this beam fail?

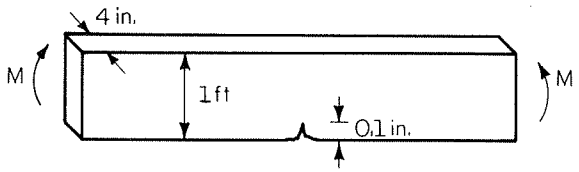

3.4. The fracture toughness of a material decreases, often dramatically, as the yield strength of the material increases. For example, for the titanium–aluminum alloy, Ti–6Al–4V, with a yield stress of 130 ksi, the fracture toughness is 105 ksi $\sqrt{\text{in.}}$ If the yield stress is increased to 150 ksi, the fracture toughness decreases to 50 ksi $\sqrt{\text{in.}}$

An engineer is faced with the following problem. His company has been manufacturing a component in the shape of a large sheet or plate using the alloy above in the 130-ksi yield strength condition. It has been suggested to him that a weight reduction could be obtained by using the alloy in the 150-ksi yield strength condition. Nondestructive testing of this component can reliably detect an edge crack of 0.2 in. Thus design requirements specify that the critical edge crack size be larger than this value (0.2 in). In addition, a factor of safety of 2 is specified for the design stress. (The design stress must be less than or equal to one-half the yield stress.) He has been asked to evaluate the proposed change in material. Should he approve the proposed change? Verify with calculations and comments. What is the maximum design stress that could be used with the higher strength material? Would use of the higher strength material result in a weight reduction?

3.5. A large cylindrical bar made of 4140 steel ($\sigma_y = 90$ ksi) contains an embedded circular (penny shaped) crack with a 0.1 in. diameter. Assume that the crack radius, a, is much smaller than the radius of the bar, R, so that the bar may be considered infinitely large compared to the crack. The bar is subjected to a tensile stress of 50 ksi. Determine the plastic zone size at the crack tip. Are the basic LEFM assumptions violated?

3.6. A large plate made of 4140 steel ($\sigma_y = 90$ ksi) containing a 0.2 in. center crack is subjected to a tensile stress of 30 ksi. Determine the plastic zone size. Are LEFM assumptions violated? If the yield strength of the material is reduced by a factor of 2, calculate the plastic zone size. Are LEFM assumptions violated? Discuss the relationship between yield strength and plastic zone size. What effect does the thickness of the plate have on the plastic zone size?

3.7. If the plate in Problem 3.6 was made from the material with the lower yield strength and subjected to a reversed stress of 30 ksi, calculated the reversed plastic zone size. Are LEFM assumptions violated? Discuss.

3.8. Fracture toughness often decreases significantly with decreasing temperature. As an example of this, the fracture toughness of A27 cast steel is plotted versus temperature (°F) below. (Data taken from Ref. 54.)

A component, which can be modeled as a beam subjected to a bending moment, is made from this material and experiences temperatures ranging from −150 to +150°F. Quality control procedures can only ensure that the component will have no cracks larger than 0.4 in. Assume that the crack length is much smaller than the beam depth. Determine the maximum bending moment that this component may withstand for a beam depth of 6 in. and a thickness of 3 in.

3.9. A very wide plate made from Al 7075-T651 ($K_{Ic} = 27$ ksi $\sqrt{\text{in.}}$, $\sigma_y = 80$ ksi) contains an edge crack. Plot the allowable nominal stress (ksi) as a function of crack size, a (in inches), if the design requirements specify a factor of safety of 2 on the critical stress intensity factor. If the plate specifications were changed so that Al 7050-T73651 was used ($K_{Ic} = 35$ ksi $\sqrt{\text{in.}}$, $\sigma_y = 70$ ksi), replot the curve. For a nominal stress of one-half the yield stress, determine the increase in allowable flaw size by changing from the Al 7075 alloy to the Al 7050 alloy.

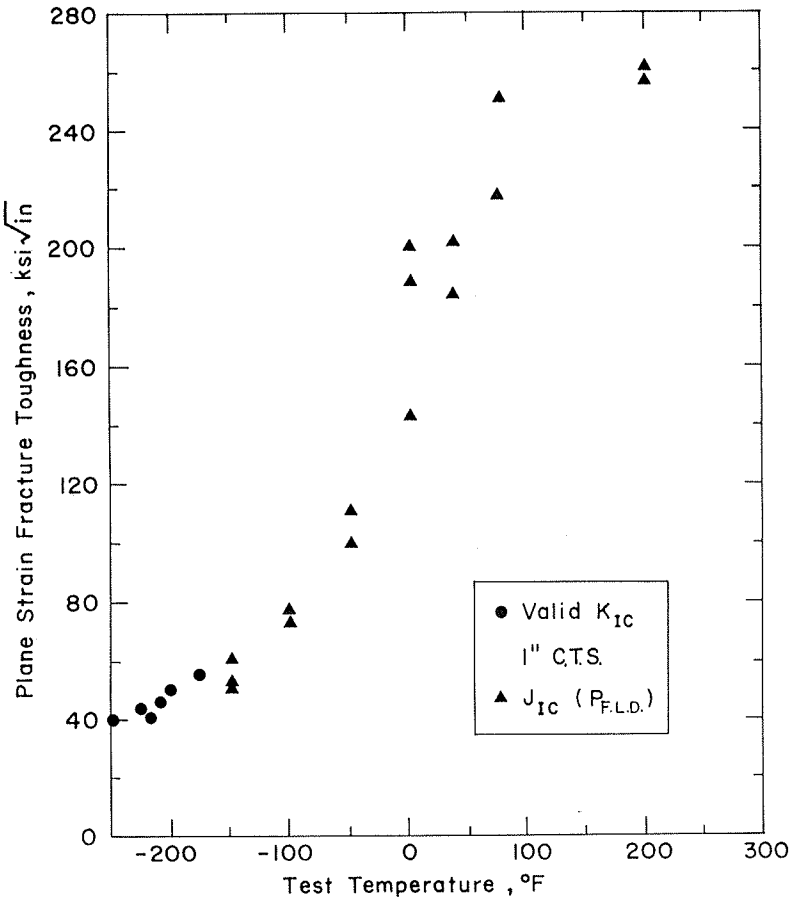

Figure P3.8

3.10. Design a pressure vessel that is capable of withstanding a static pressure of 1000 psi and that will "leak-before-burst." The required material has a fracture toughness of 60 ksi $\sqrt{\text{in.}}$ and a yield strength of 85 ksi. The diameter of the vessel is specified to be 4 ft. A crack with surface length of 1 in. can reliably be detected. Since the cost of the vessel is related directly to the amount of material used, optimize the design so that the cost is minimized.

SECTION 3.3

3.11. The crack in an edge-cracked plate extends due to repeated loading. The crack is initially 0.01 in. and the plate width is 5 in. Calculate the geometry correction factor, $f(g)$, for crack lengths of 0.01, 0.05, 0.1, and 0.2 in. Discuss the amount of error that

would be introduced in the fatigue crack growth calculation in assuming that the geometry correction factor remained constant for the interval $a = 0.01$ to 0.2 in.

Discuss the impact of this on the method of crack growth predictions outlined in Section 3.3.2. Discuss the amount of error that would be introduced if the initial crack length were assumed to be 0.2 in. instead of 0.01 in.

3.12. A component made from 7005-T53 aluminum contains a semi-circular surface crack ($a/c = 1$) and is subjected to $R = 0.1$ loading with a stress range, $\Delta\sigma$, of 250 MPa. (Refer to Example 3.1 for an expression for the stress intensity range, ΔK.) The following crack growth data were obtained in laboratory air environment. Using these data:

(a) Plot crack length, a (mm), versus cycles, N.

(b) Plot da/dN versus ΔK. Identify the three regions of crack growth.

(c) Determine the Paris law constants, C and m, for the linear region of crack growth.

N (cycles)	a (mm)	da/dN (mm)
95,000	0.244	
100,000	0.246	7.00×10^{-7}
105,000	0.251	3.920×10^{-6}
110,000	0.285	9.665×10^{-6}
115,000	0.347	1.053×10^{-5}
125,000	0.414	1.230×10^{-5}
130,000	0.490	2.063×10^{-5}
135,000	0.621	4.661×10^{-5}
140,000	0.956	9.565×10^{-5}
145,000	1.577	3.964×10^{-4}
147,000	2.588	1.105×10^{-3}
147,400	3.078	1.554×10^{-3}
147,500	3.241	8.758×10^{-3}
147,500	3.445	

3.13. The following crack growth data were obtained from a center-cracked panel subjected to a stress range of 50 ksi. Plot the crack size, a, as a function of life, N. Determine the crack growth rate da/dN. Plot da/dN as a function of ΔK and determine the Paris constants. Compare the da/dN values calculated to the following values given. How sensitive are the Paris constants to the da/dN values?

3.14. An aluminum alloy has the following fatigue crack propagation relationship for $R = 0$ loading:

$$\frac{da}{dN} = 10^{-8}(\Delta K)^4 \quad \text{in./cycle}$$

A component that is made from this material is subjected to 0.1 Hz, constant amplitude, zero to maximum loading in service. The component is inspected every

FOR PROBLEM 3.14 TABLE FOR 3.13

Cycles	Crack Length (in.)	da/dN (in./cycle)
10,000	0.009	
20,000	0.010	1.56×10^{-7}
30,000	0.012	2.46×10^{-7}
40,000	0.015	5.10×10^{-7}
50,000	0.018	4.50×10^{-7}
60,000	0.025	1.05×10^{-6}
70,000	0.040	1.74×10^{-6}
80,000	0.060	2.94×10^{-6}
90,000	0.100	6.81×10^{-6}
100,000	0.200	

1000 hours using a facility capable of detecting a crack of 0.2 in. length on the surface. In rare cases where the failure occurred in service, the crack was found to be semi-circular with a depth of 1 in. ($a = 1$ in.). Assuming that the aspect ratio remains equal to 1 ($a/c = 1$) throughout the life, determine the limit of ΔS_{max} for the inspection program to be successful. Assume that the crack depth is much smaller than the thickness of the part so that the backwall effect may be ignored. (*Hint*: See Example 3.1 for the stress intensity factor.)

A new inspection technique promises to reduce the minimum detectable crack by a factor of 10. Estimate how much the inspection interval can be increased and still assure safe operation in service without changing the stress. How much could ΔS_{max} be increased if the new facility were used with the original inspection interval?

3.15. A component made from A27 cast steel was inspected and found to have a circular corner crack with a radius of 0.1 in. The fracture toughness for this material at the operating temperature (75°F) is about 220 ksi $\sqrt{\text{in.}}$ Using the da/dN versus ΔK curve shown below [54], determine the number of constant amplitude cycles of 50 ksi (zero-to-maximum loading) that the component may experience before fast fracture. Assume that the crack size is negligible compared to the thickness throughout the life of the component. (*Hint*: See Example 3.1 for the stress intensity.)

If the operating temperature were decreased to 0°F, so that the fracture toughness was 120 ksi $\sqrt{\text{in.}}$, determine the number of cycles before failure. (Assume that the crack growth rate remains constant with temperature.) How does the final crack size, a_f, affect the number of cycles that this component may experience?

3.16. A very wide plate containing a central crack of length $2a$ is made of a material with a yield strength of 70 ksi and a fracture toughness of 100 ksi $\sqrt{\text{in.}}$ The plate is subjected to a zero-to-maximum constant nominal stress range. Assuming that the plate fails catastrophically when $K_{max} = K_{Ic}$, determine the number of cycles to failure for $S_{max} = 20$, 30, 40, 50, and 60 ksi for initial crack lengths of $a_0 = 0.005$, 0.01, 0.05, and 0.1 in. The crack growth constants for the Paris law equations are

$$C = 10^{-8} \qquad m = 3$$

Plot the results as a S–N curve with a_0 as the parameter.

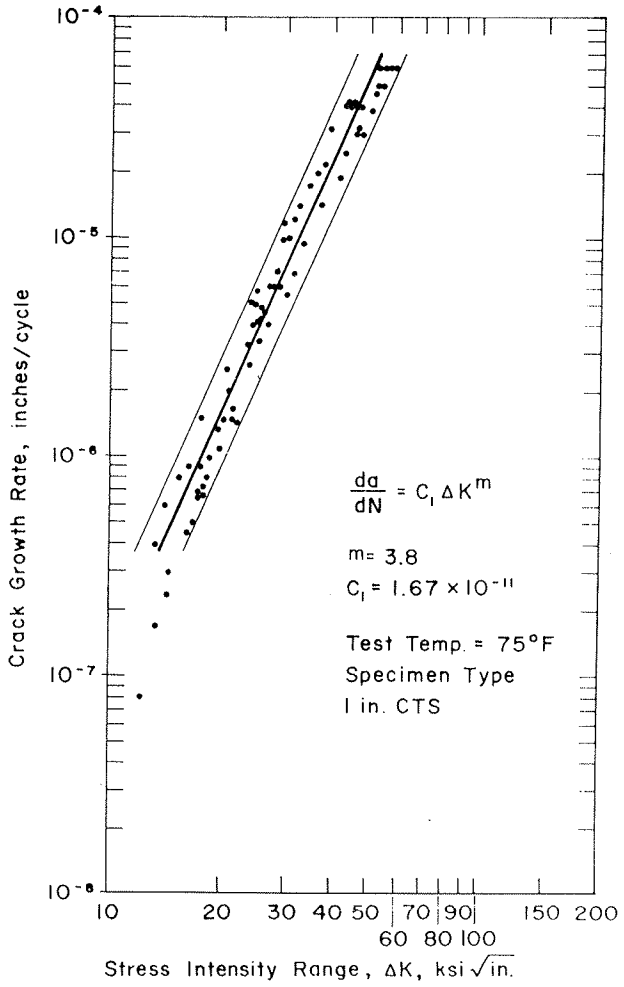

Figure P3.15

3.17. A surface crack of 0.1 in. depth and 0.2 in. surface length is found in a thick component. The component is scheduled to be repaired in 6 months. From loading and material information, it has been determined that catastrophic failure will occur when the crack size reaches 0.5 in. in depth. The component is subjected to zero-to-maximum loading 10 times per hour, with the maximum stress equal to 50 ksi. Assuming that the crack ratio remains constant, will the component fail before repair? (Assume that the crack growth rate, da/dN, calculated for $a = 0.1$ in. remains constant until the crack length reaches $a = 0.2$. Then assume that the crack growth remains constant until the crack increases by another 0.1 in. Continue to use this assumption to determine the number of cycles that the component may withstand before failure.) $C = 6 \times 10^{-6}$, $m = 3$.

3.18. If the beam in Problem 3.3 was subjected to the loading histories shown below, determine the stress intensity factor ranges, ΔK, for each history and discuss which history would be more damaging (neglect crack closure effects). Determine the stress ratio, R, for these two histories. Discuss the effect that crack closure would have on the damage produced by the two histories.

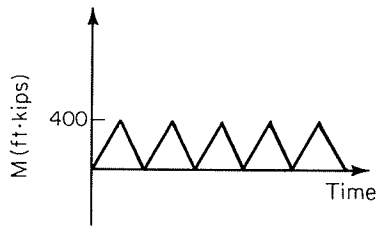

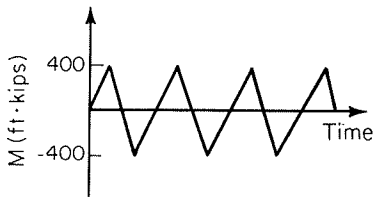

Moment vs Time Loading Histories

Figure P3.15

found in a thick
hs. From loading
failure will occur
is subjected to
n stress equal to
e component fail
ed for $a = 0.1$ in.
me that the crack
. Continue to use
component may